7th International Conference on Crack Paths

Mixed modes crack paths in SCB specimens obtained via SLS

Liviu Marsavina[a], Dan Ioan Stoia[a]*, Emanoil Linul[a]

[a] Department of Mechanics and Strength of materials, University Politehnica Timisoara,

Blvd. M. Viteazul, No. 1, 300222 Timisoara, Romania

Abstract

The paper presents experimental results of the crack path in Semi-Circular Bend (SCB) specimens obtained through additive manufacturing using Selective Laser Sintering (SLS) process. Determination of fracture parameters for components obtained via Additive manufacturing is a challenging topic, due to the influence of manufacturing parameters on the mechanical properties. Several researches provided the fracture toughness of SLS components, however there are not yet available results regarding the crack paths in such materials. The SCB specimens were designed with different crack orientations (0°, 15°, 30°, 45°, and 54°) and manufactured using EOS Formiga – SLS equipment (energy density 0.066 J/mm2, chamber temperature 169.5 °C, layer thickness 0.1 mm) using PA2200 material. The specimens were tested in symmetric three point bending configuration, creating 6 mode mixity from mode I (0° – crack orientation) to pure mode II (54° – crack orientation). Tests were performed at room temperature using 2 mm/min loading speed in a Zwick ProLine Z005 testing machine. For each crack orientation five specimens were tested. Crack initiation angle and crack propagation were measured by image digitization after the mechanical testing and presented in accordance to the initial orientation of the crack. Also, numerical simulation of crack path was conducted in the same way like the experiment and results were compared to the measured one.

Keywords: selective laser sintering, polyamide, crack initiation angle, crack path;

* Corresponding author.
E-mail address: liviu.marsavina@upt.ro

1. Introduction

Selective laser sintering (SLS) is an additive manufacturing (AM) process where raw material in the powder form is thermal binding using an electrical heating system and a laser beam. The powder-laser interaction, electrostatic charge of polymer particles, powder humidity and cleanliness are highly influencing the neck formation between individual particles. This leads to structural defects that further influence the mechanical and geometrical properties of laser sintered components as Tan (2020), Xie (2021), Petzold (2019) presented. Among the mechanical properties affected by the structural defects or structural particularities generated by the process, the fracture mechanics behavior of AM parts is less studied (Brugo (2016), Crespo (2017), Berto (2020)), in particular mixed mode I/II cracking of AM materials, Ameri (2021).

Many authors use semi-circular bending (SCB) specimen for experimentally determining the fracture behavior of various brittle materials. The advantages of SCB are the simple geometry of it, the simple manufacturing especially by AM and the simple loading fixtures (compressive load) as Aliha (2011), Mubaraki (2020), Ayatollahi (2006) presented. In addition, when preparing the SCB samples by AM, the orientation of the initial crack from pure mode I up to pure mode II can be easy controlled trough the design of the sample.

The crack initiation angle and crack path can be investigated both by geometric measurements on the tested specimens or by numerical simulation conducted in the same conditions as Marsavina (2015) and Li (2013) presented. Determining angles and trajectories by image digitization imply errors coming from image resolution and dimensional scale association.

The purpose of the study was to determine the crack initiation angles and crack paths in selective sintered polyamide PA2200 starting from an initial crack orientation of 0°, 15°, 30°, 45°, and 54°, and to identify the effect of layer manufacturing on these fracture parameters.

Nomenclature	
SLS	selective laser sintering
AM	additive manufacturing
SCB	semi-circular bending
α	initial crack orientation
θ	crack initiation angle
$F_{max.}$	maximum force
δ	displacement
a	notch length
R, B	radius and thickness of the specimen
S	span between pins

2. Materials and methods

2.1. Sample design and manufacturing

The design of the SCB sample was made in SolidWorks 2020 (3DS North American HQ, USA). The initial crack length and orientations were constructed directly in the design phase, so that no further processing after the additive process is required. The size, shape and orientations of the initial crack can be observed in the figure 1 a.

The manufacturing process was conducted on EOS Formiga P100 (Electro Optical Systems - EOS GmbH, Krailling, Germany) using the PA2200 powder commercially available from the same company. The parts positioning in the building envelope is presented in the figure 1 b, where the orientation of the initial crack in relation to the manufacturing layer can be also observed. A total number of 25 samples were built in the same conditions, using the following parameters: energy density 0.066 J/mm^2, beam offset 0.15 mm, chamber temperature 169.5 °C, removal chamber temperature 152 °C, layer thickness 0.1 mm, scaling factors 2.2% and X-Y alternating hatching strategy, as Stoia et al (2020) and Stoia et al (2019) presented.
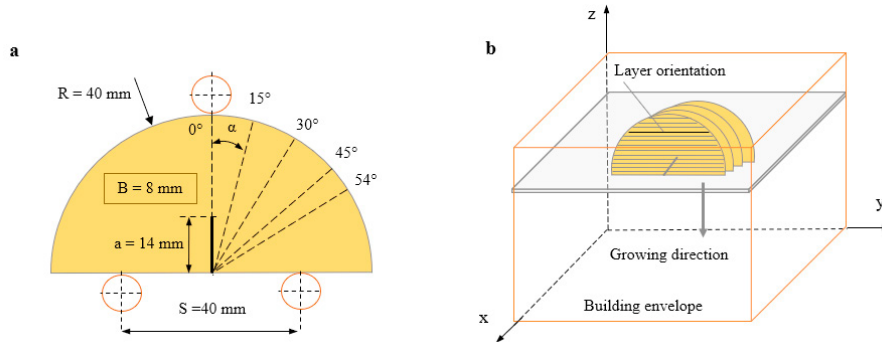
Fig. 1. Sample design and manufacturing preparation: (a) Sample size and shape; (b) Samples positioning.

2.2. Mechanical testing

The mechanical testing was carried on 5 kN Zwick machine, using a 3-point bending fixture. The span of bottom pins was set to 40 mm while the upper loading pin was placed in the middle opening between pin supports was 80 mm and the loading pin was placed in the middle of the opening. All tests were conducted under the same conditions of 5 mm/min velocity and an acquisition sampling rate of 600 Hz.

2.3. Image digitization and crack measurements

All broken samples were then arranged on a flat surface together with a ruler of 0.5 mm resolution. Images of all samples were taken using a photo-camera with a resolution of 40 mega pixel. The image processing was done in ImageJ (Image processing and analysis in Java) free software by importing first the photographs, setting the scale in accordance to the attached ruler and then measuring the initiation angle and the crack path. The measurements of crack initiation angle were done five times on every individual sample, in order to compute an average angle that prevents as much as possible the human error from data.

2.4. Numerical simulation of fracture

The numerical simulation was conducted using FRANC2D software. The SCB specimens with crack length of 14 mm and different crack orientations α were modeled under Plain Stress conditions with 8 mm thickness (similar with the experiment). A linear elastic material model with Young modulus 1200 MPa and Poisson ratio $v=0.4$ was considered. The symmetric three-point bend boundary conditions were applied, replicating the experimental set-up. The models were meshed with isoparametric 8 node specimens and at the crack tip singular 6 node elements were imposed, collapsing 3 nodes at the crack tip and moving the middle nodes at one quarter of element size for the edges radiating from the crack tip. For the crack propagation study the J-Integral method was used to calculate the stress intensity factors, a step increment of 0.5 mm was chosen for the crack increment and the automatic remesh and fill algorithm for crack propagation, Iesulauro (2014). The maximum circumferential stress criterion was considered for calculating the crack propagation angle.

3. Results and discussions

The mechanical testing finalizes with force-displacement curves of every individual samples. The failed specimens (representative pictures) can be observed in the figure 2. Here, the 0° initial crack orientation led to a quasi-vertical crack path (pure mode I) while the other initial orientations tend to mode I by an arch trajectory of crack propagation. In some samples, especially on the pure mode II, a layer propagation of crack was observed (figure 2 e and f). This may be explained by lower mechanical bonding at interlayer than intralayer.

The investigation on initial crack angles was done by measuring the angles of five directions in the vicinity of the crack tip (figure 3). The values were then extracted and averaged in order to determine one single angle value that characterizing one sample. The standard deviation of the angles was in the range of 2.4 up to 9.2 degrees, the lowest value corresponding to pure mode I while large variability vas recorded for 15° initial orientation.

In figure 4 could be seen the crack propagation paths resulted from numerical simulation for the crack orientation α at 15°, 30°, 45° and 54°.
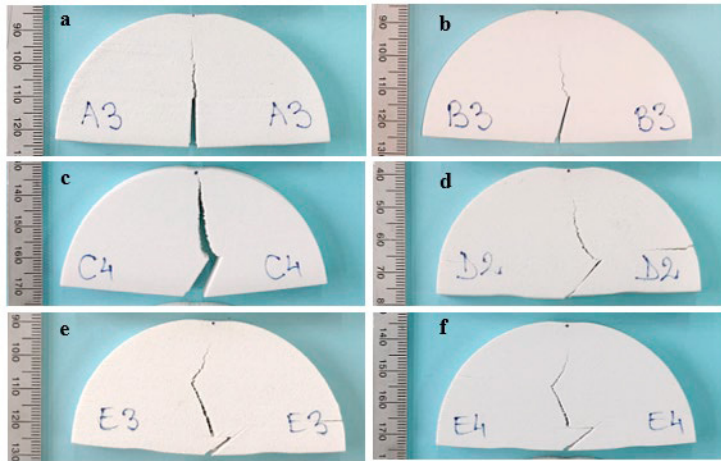

Fig. 2. Representative SCB samples after mechanical testing: (a) 0°; (b) 15°; (c) 30°; (d) 45°; (e, f) 54°.
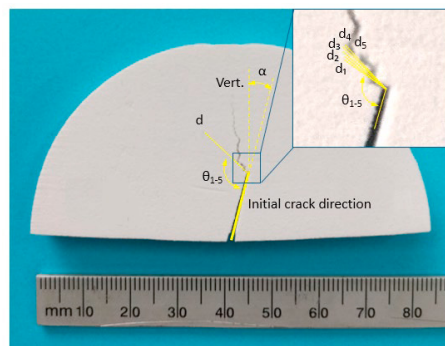

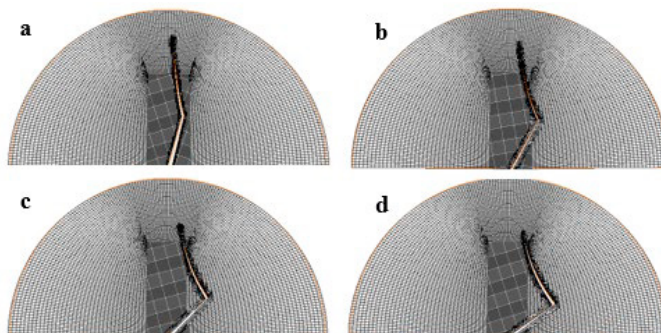Fig. 3. Multiple measurements of crack initiation angle on one SCB sample.

Fig. 4. Simulation images of crack propagation: (a) 15°; (b) 30°; (c) 45°; (d) 54°.

The figure 5 presents the representations of crack paths of experimental samples and of numerical simulations. It is clearly observable the curvature differences between the corresponding paths of the two images. The simulation indicates a smooth transition, characterized by large radius, from the mixed mode to the pure mode I track, while in the experiments the curvature of smaller radius followed by steeper slopes can be identified. Even some horizontal trajectory of crack (figure 5 a, α4 series) can be observed for the pure mode II, which denote a short domain of interlayer failure of the sample.

The crack initiation angle in accordance to the initial crack orientation is compared with two classical fracture criteria:

-   maximum circumferential stress (MTS), Erdogan and Sih (1963):

$$\theta_c = -\arccos\left(\frac{3K_{II}^2 + K_I\sqrt{K_I^2 + 8K_{II}^2}}{K_I^2 + 9K_{II}^2}\right) \tag{1}$$

-   equivalent stress intensity factor (ESIF) Richard (1985)

$$\theta_c = \mp\left(155.5^0\frac{|K_{II}|}{|K_I| + |K_{II}|}\right) - 83.4^0\left(\frac{|K_{II}|}{|K_I| + |K_{II}|}\right)^2 \tag{2}$$

In figure 6 the comparison between experimental and prediction of crack initiation angle could be observed. Very good agreement could be seen for the MTS criterion and reasonable for ESIF criterion, which allow to conclude that the classical fracture criteria could be applied successfully for SLS manufactured specimens. For the experimental measured crack initiation angle the standard deviation is high (around 15 %) but almost constant for the samples of 0°, 30°, 45°, and 54° and significant different for 15° samples (28%). This high variability of data for α = 15° can be put on layer delamination. This initial crack direction is very close to the vertical direction (0°, pure mode I) so it seems that the instant preferred direction of crack initiation is sometimes the direction of the first encountered layer. Some other times, the fracture path propagates trough the intralayer domain without encountering delamination. So, an instability of crack initiation for this angle can be identified.
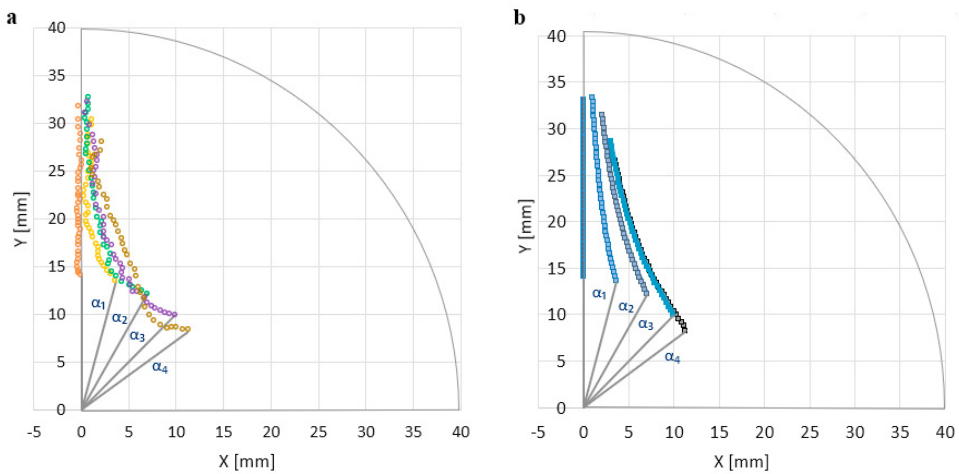

Fig. 5. Measured crack paths (a) and simulated crack paths (b) according to the same initial crack orientation.
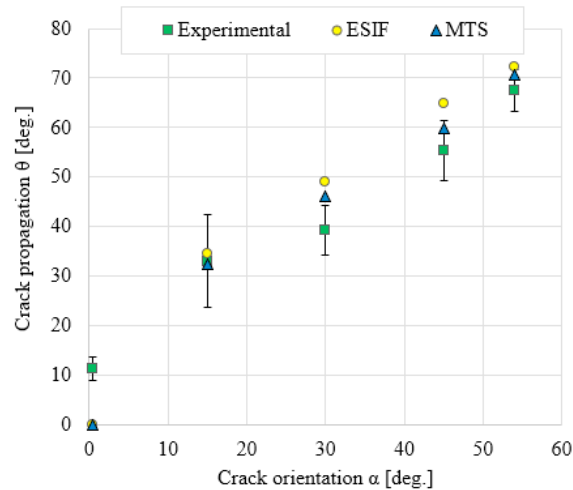
Fig. 6. Crack initiation angle (θ) according to the initial crack orientation angle (α).

4. Conclusions

The paper presents a study on the crack path of laser sintered polyamide PA2200 under mixed mode loading. Relying on SCB design, the study was conducted on 25 samples possessing the initial crack orientation angles of 0°, 15°, 30°, 45°, and 54°. The investigations focus on determining the crack initiation angle and the crack path in accordance to the initial orientation of crack. In addition, numerical simulation of crack propagation was presented for comparing the theoretical crack path with the experimental data. The conclusions of the study can be summaries as:

- Crack initiation angle could be predicted by classical fracture criteria (MTS and ESIF),
- The crack initiation angle has to be computed as an average from multiple angular measurements,
- Some samples experience delamination, so the crack is propagating for a short distance on layer,
- The observations of this study are valid only on additive manufactured samples by selective laser sintering growth vertically resulting a layered structure (figure 1),
- The instability of crack initiation for 15° initial crack orientation was identified,
- The crack propagation paths could be simulated using the remesh and fill algorithm and MTS criterion for crack propagation angle considering the material isotropic and homogeneous.

Acknowledgements

References

Aliha, M.R.M., Ayatollahi, Majid R., 2011. Mixed mode I/II brittle fracture evaluation of marble using SCB specimen. Procedia Engineering. 10, 311–318.
Ameri, B., Taheri-Behrooz, F., Aliha, M.R.M., 2021. Evaluation of the Geometrical Discontinuity in the Mixed-Mode I/II Fracture Load of FDM 3D-Printed Parts. Theoretical and Applied Fracture Mechanics. 113.
Ayatollahi, M.R., Aliha, M.R.M., 2007. Fracture toughness study for a brittle rock subjected to mixed mode I/II loading. International Journal of Rock Mechanics & Mining Sciences. 44, 617–624.
Ayatollahi, M.R., Aliha, M.R.M., Hassani, M.M., 2006. Mixed mode brittle fracture in PMMA—An experimental study using SCB specimens. Materials Science and Engineering A. 417, 348–356.

Berto, M.R., Khosravani, F., Ayatollahi, M.R., Reinicke, T., 2020. Fracture behavior of additively manufactured components: A review, Theor. Appl. Fract. Mech. 109, 102763.

Brugo, T., Palazzetti, R., Ciric-Kostic, S., et al., 2016. A. Fracture mechanics of laser sintered cracked polyamide for a new method to induce cracks by additive manufacturing, Polym. Test. 50, 301-308.

Crespo, M., Gómez-del Río, M.T., Rodríguez, J., 2017. Failure of SLS polyamide 12 notched samples at high loading rates, Theor. Appl. Fract. Mech. 92, 233-239.

Erdogan, F., Sih, GC., 1963. On the crack extension in plates under plane loading and transverse shear. J Basic Engn. 85, 519-525.

Iesulauro, E., 2004. FRANC2D/L: A Crack Propagation Simulator for Plane Layered Structures, Version 1.5 User's Guide, Cornell University

Li, C., Xie, L., Ren, Li., Xie, H., Wang, J., 2013. Evaluating the Applicability of Fracture Criteria to Predict the Crack Evolution Path of Dolomite Based on SCB Experiments and FEM. Mathematical Problems in Engineering. 2013, 1-13, 10.1155/2013/959806.

Linul, E., Marsavina, L., Stoia, D.I., 2020. Mode I and II fracture toughness investigation of Laser-Sintered Polyamide, Theor. Appl. Fract. Mech., 106, 1-11.

Marsavina, L., Linul E., Voiconi, T., Constantinescu, D., Apostol, D., 2015. On the crack path under mixed mode loading on PUR foams. Frattura ed Integrità Strutturale. 9, 10.3221/IGF-ESIS.34.43.

Mubaraki, M., Sallam, H., 2020. Reliability study on fracture and fatigue behavior of pavement materials using SCB specimen. International Journal of Pavement Engineering. 10, 1080/10298436.2018.1555332.

Petzold, S., Klett, J., Schauer, A., Osswald, A., 2019. Surface roughness of polyamide 12 parts manufactured using selective laser sintering. Polymer Testing. 80, 106094.

Richard, H.A., 1985. Bruchvorhersagen bei uberlagreter normal- und schubbeanspruchung von rissen, VDI-Verlag, Dusseldorf.

Stoia, D.I., Marsavina, L., Linul, E., 2021. Mode I critical energy release rate of additively manufactured polyamide samples, Theor. Appl. Fract. Mech. 114, 1-10.

Stoia, D.I.; Marsavina, L.; Linul, E., 2020. Mode I Fracture Toughness of Polyamide and Alumide Samples obtained by Selective Laser Sintering Additive Process. Polymers. 12, 640.

Stoia, D.I., Linul, E., Marsavina, L., 2019. Influence of manufacturing parameters on mechanical properties of porous materials by Selective Laser Sintering, Materials. 12, 871.

Tan, L.J., Zhu, W., Sagar K., Zhou, K., 2020. Comparative study on the selective laser sintering of polypropylene homopolymer and copolymer: processability, crystallization kinetics, crystal phases and mechanical properties. Additive Manufacturing. 37, 101610. 10.1016/j.addma.2020.101610.

Xie, D., Dittmeyer, R., 2021. Correlations of laser scanning parameters and porous structure properties of permeable materials made by laser-beam powder-bed fusion. Additive Manufacturing. 47, 102261, ISSN 2214-8604.